Geochemical Perspectives Letters EAG

Pyrite Re-Os dating confirms synchronous magmatism and hydrothermalism in Troodos ophiolite

B.-X. Su[1,2*], B.-Y. Gao[1], S. Ning[1,2], V. Symeou[3]

Abstract

https://doi.org/10.7185/geochemlet.2629

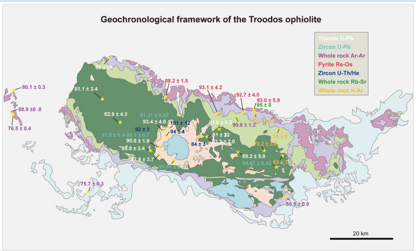

The Troodos ophiolite in Cyprus represents one of the best preserved ophiolites globally, yet its precise formation time scale remains debated. This study presents the first Re-Os isochron dating of pyrite from four Cyprus-type sulfide deposits (Agrokipia, Memi, Kokkinopezoula, and Apliki) hosted within the Troodos pillow lava sequence. The results yield ages of 93.0 ± 5.9 Ma, 93.1 ± 4.2 Ma, 92.7 ± 4.0 Ma, and 88.2 ± 1.5 Ma, respectively, directly constraining the timing of seafloor hydrothermal mineralisation. These ages, combined with recently published high precision U-Pb zircon/titanite ages from plutonic and sheeted dike rocks, reveal that (1) the main phase of crustal accretion and high temperature hydrothermal activity occurred synchronously at ~93–90 Ma, (2) post-accretion low temperature alteration and cooling persisted until ~74 Ma, and (3) localised magmatism continued episodically to ~81 Ma, with minor boninitic activity as late as ~55 Ma. This refined geochronological framework indicates that the Troodos ophiolite formed during a brief (~3 Myr) episode of subduction-initiation related spreading, followed by prolonged thermal evolution. The sulfide deposits serve as precise chronometers for fossil seafloor hydrothermal systems, providing critical new constraints on tectonic evolution of ophiolites worldwide.

Received 5 May 2026 | Accepted 13 July 2026 | Published 2 September 2026

Introduction

The Troodos ophiolite in Cyprus is one of the best preserved ophiolites in the world and was established as the global standard for ophiolite definition at the 1972 Penrose Conference on Ophiolites. Clarifying the spatiotemporal formation framework of the Troodos ophiolite is crucial for a comprehensive understanding of other ophiolites worldwide and the formation and evolution of ancient oceanic lithosphere (Dilek and Furnes, 2009). Prior to the 21st century, dating work on the Troodos ophiolite utilised mainly K-Ar (*e.g.*, 75–85 Ma; Desmet *et al.*, 1978; Delaloye and Desmet, 1979; Delaloye *et al.*, 1980; Staudigel *et al.*, 1986), Rb-Sr (74–95 Ma; Staudigel *et al.*, 1986; Kawahata and Scott, 1990), and biostratigraphy (75–98 Ma; Mantis, 1971; Desmet, 1977; Blome and Irwin, 1985) methods, generating large uncertainty. Subsequently, multiple conflicting models based on different ages have been proposed to explain the formation setting and tectonic evolution of the Troodos ophiolite (Moores *et al.*, 1984; Pearce and Robinson, 2010; Robertson *et al.*, 2024).

With technical development of Ar-Ar and U-Pb geochronology, it is now well established that plagiogranites in the Troodos ophiolite have consistent zircon/titanite U-Pb dates of 90.1–91.8 Ma (Mukasa and Ludden, 1987; Konstantinou *et al.*, 2007; Chen *et al.*, 2020; Su *et al.*, 2025), with an outlier of 83 Ma from zircon U-Th/He dating (Morag *et al.*, 2016), and that gabbros have zircon/titanite U-Pb dates of 91.2–93.4 Ma (Su *et al.*, 2025) with two zircon U-Th/He dates of 94 and 101 Ma (Morag *et al.*, 2016). Large age variations are observed on diabases (zircon/titanite U-Pb 81.0–94.5 Ma; Su *et al.*, 2025) and particularly pillow lavas (whole rock Ar-Ar 55.5 and 90.6 Ma; Osozawa *et al.*, 2012; titanite U-Pb 83 Ma; Su *et al.*, 2025). As a consequence, the early magmatic activity, represented by the gabbros and plagiogranites at the base of the crustal sequence in the Troodos ophiolite, has a relatively consistent age, whereas the termination time of the magmatic activity has not yet been constrained. This data set indicates that the magmatism forming the crustal sequence of the Troodos ophiolite may have lasted tens of million years, which challenges the hypothesis of rapid formation (several Myr) of this subduction-initiated ophiolite as well as others worldwide (Whattam and Stern, 2011). Precise dating of the pillow lavas that represent the final stages of magmatism is particularly important for constraining the time interval of ophiolite formation.

The pillow lavas in the Troodos ophiolite feature boninitic or arc tholeiitic compositions and variable degrees of alteration, resulting in a lack of suitable mineral targets for dating. Notably, many sulfide deposits are hosted within pillow lava series (Constantinou and Govett, 1973) and represent fossil seafloor hydrothermal systems formed during ophiolite crustal construction (Adamides, 2010; Kawahata and Scott, 1990). The sulfide minerals in these deposits are well preserved, free of alteration, which makes them good potential targets for Re-Os isochron dating. In this study, we separated pyrite in volcanic rocks and sulfide ores from four sulfide deposits and measured their Re

1. State Key Laboratory of Lithospheric and Environmental Coevolution, Institute of Geology and Geophysics, Chinese Academy of Sciences, Beijing 100029, China
2. University of Chinese Academy of Sciences, Beijing 100049, China
3. Cyprus Geological Survey, 1 Lefkonos St., 2064 Strovolos, Nicosia, Cyprus
* Corresponding author (email: subenxun@mail.igcas.ac.cn)

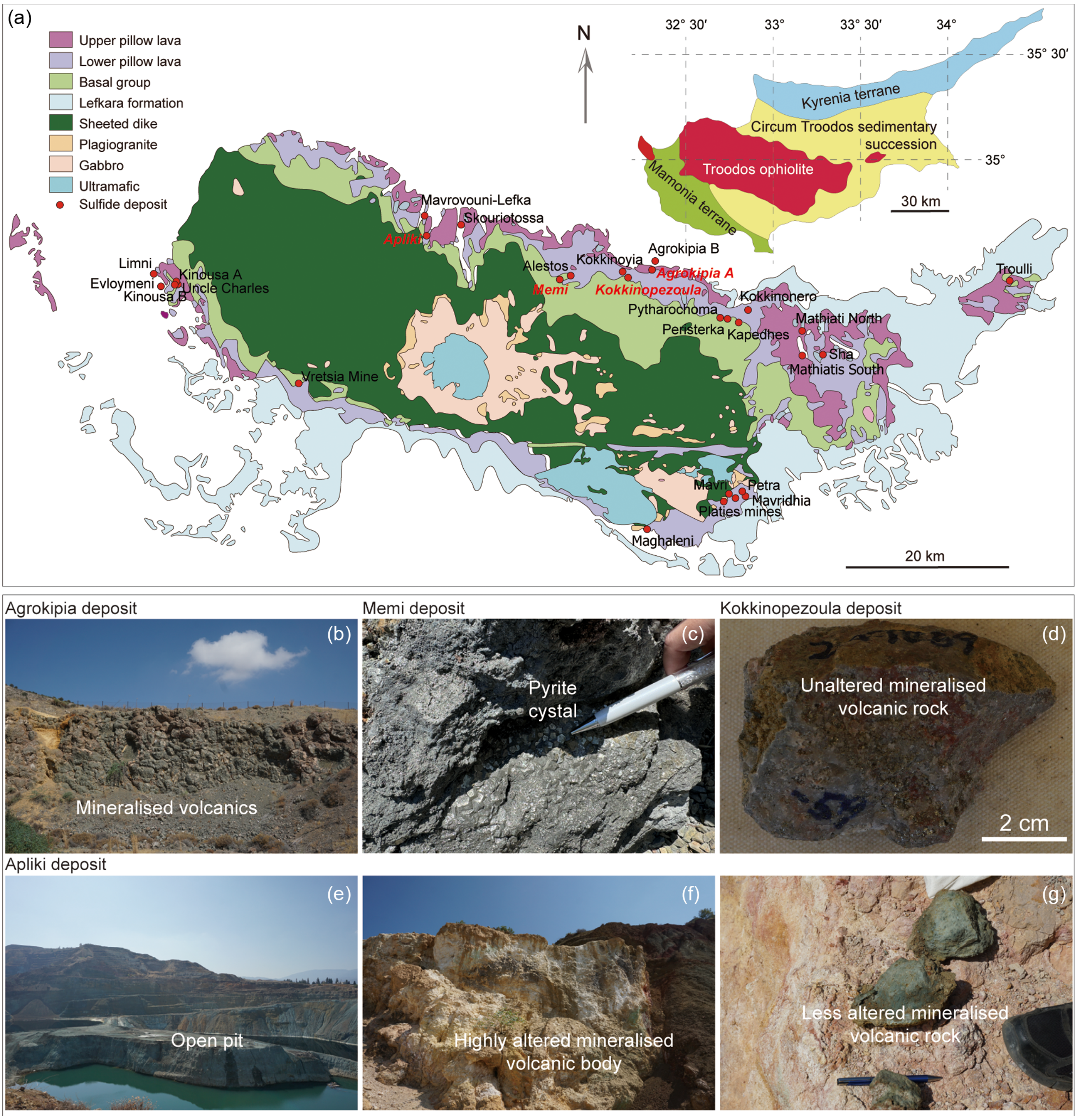

Figure 1 (a) Geological map of the Troodos ophiolite (modified after Geological Survey Department, Cyprus, 2016) showing distribution of sulfide deposits. The studied sulfide deposits are highlighted in bold red italic text. Field exposures of sulfide deposits including **(b)** mineralised volcanics in Agrokipia, **(c)** pyrite ores in Memi, **(d)** unaltered mineralised volcanic rock in Kokkinopezoula, **(e)** open pit and **(f, g)** alteration of volcanic rocks in Apliki.

and Os isotope compositions, which we use to determine their formation ages (see analytical methods in Supplementary Information). These age data, together with those in the literature, are used to further constrain the geochronological framework of the Troodos magmatism.

Sulfide Deposits in the Troodos Ophiolite

The Troodos ophiolite preserves a nearly complete section of Cretaceous oceanic crust (ultramafics, gabbros, sheeted dikes, and pillow lavas) (Geological Survey Department, Cyprus, 2016). The sulfide deposits are an integral part of the volcanic section and are classic Cyprus-type volcanogenic massive sulfide (VMS) deposits (Constantinou and Govett, 1973). They occur at various stratigraphic levels but are most common near the top of the Lower Pillow Lavas or at the Lower-Upper Pillow Lava contact (Adamides, 2010) (Fig. 1a). Approximately 20–30 significant deposits are known; most lie within a ~40 km × 20 km belt on the northern slope. They are absent or very rare on the southern flank (Fig. 1a). Their host rocks are basaltic pillow lavas, sheet flows, breccias, and hyaloclastites of island arc tholeiite to boninitic affinity (Constantinou and Govett, 1973; Adamides, 2010).

Ore bodies are typically underlain by hydrothermally altered lavas/stockwork zones and overlain by the Ochre Group (Fe-rich sediment), Upper Pillow Lava and/or Umber (Mn-rich sediment) (Constantinou and Govett, 1973). Concentrically zoned alteration pipes record fluid pathways (Richards *et al.*, 1989). From outer to inner zones, the facies transition from smectite-rich to chlorite-albite in the outer zones, to chlorite-illite/rectorite with intense leaching in the inner mineralised zones (Richards *et al.*, 1989). At the root zone, epidosites in sheeted dikes represent the deep seated sites of metal leaching (Gillis and Robinson, 1990). The dominant minerals of the ore bodies are pyrite and chalcopyrite, with minor sphalerite (Martin *et al.*, 2018). They are thought to have formed synchronously with the ophiolite itself during the Late Cretaceous, but chronological evidence is lacking.

Most sulfide deposits in Troodos ophiolite were exploited periodically between 1950–1980 and have been mined out to date. Four deposits including Agrokipia, Memi, Kokkinopezoula, and Apliki were chosen for Re-Os isochron dating in this study, and sulfide ores and sulfide-rich volcanic rocks were collected. The Agrokipia deposit is located within the Lower Pillow Lavas which in certain locations are overlain by Upper Pillow Lavas (Fig. 1b). The Memi deposit is characterised by chloritised lavas with a gossan cap, and many pyrite ores are available (Fig. 1c). The Kokkinopezoula deposit preserves unaltered mineralised volcanic rocks and ores (Fig. 1d). The Apliki deposit is controlled by a north-south fault zone, with highly to less altered mineralised volcanic rocks and rarity of ores left in the open pit (Fig. 1e-g). Despite variable alteration of the host rocks, pyrite separates are pristine, and show no evidence of post-depositional disturbance of their Re-Os isotope compositions.

Results

Pyrites from Agrokipia, Memi, and Kokkinopezoula deposits show comparable Re (<10 ng/g), common Os (<0.013 ng/g) and ^{187}Os (<0.01 ng/g) concentrations, which are significantly lower than those from Apliki deposit (Re 40–480 ng/g; common Os 0.007–0.868 ng/g; ^{187}Os 0.038–0.485 ng/g) (Table S-1). Their isotope ratios are highly variable but generally overlapped, with ^{187}Re/^{188}Os (868–23045 in the former three *vs.* 2682–57763 in Apliki) and ^{187}Os/^{188}Os (1.61–36.94 *vs.* 4.3–84.62) (Table S-1). These data yield ischron dates of 93.0 ± 5.9 Ma (2σ) for Agrokipia, 93.1 ± 4.2 Ma for Memi, 92.7 ± 4.0 Ma for Kokkinopezoula, and 88.2 ± 1.5 Ma for Apliki (Fig. 2).

Discussion

Evaluation of data quality. Pioneering work established the Re-Os technique for pyrite, demonstrating that it can directly date sulfide mineralisation (Stein *et al.*, 2000). This technique has been applied successfully to various deposits, providing precise ages for ore formation that complement indirect methods such as U-Pb zircon dating of host rocks (Li *et al.*, 2025). The method assumes that (1) all samples are cogenetic and formed from a

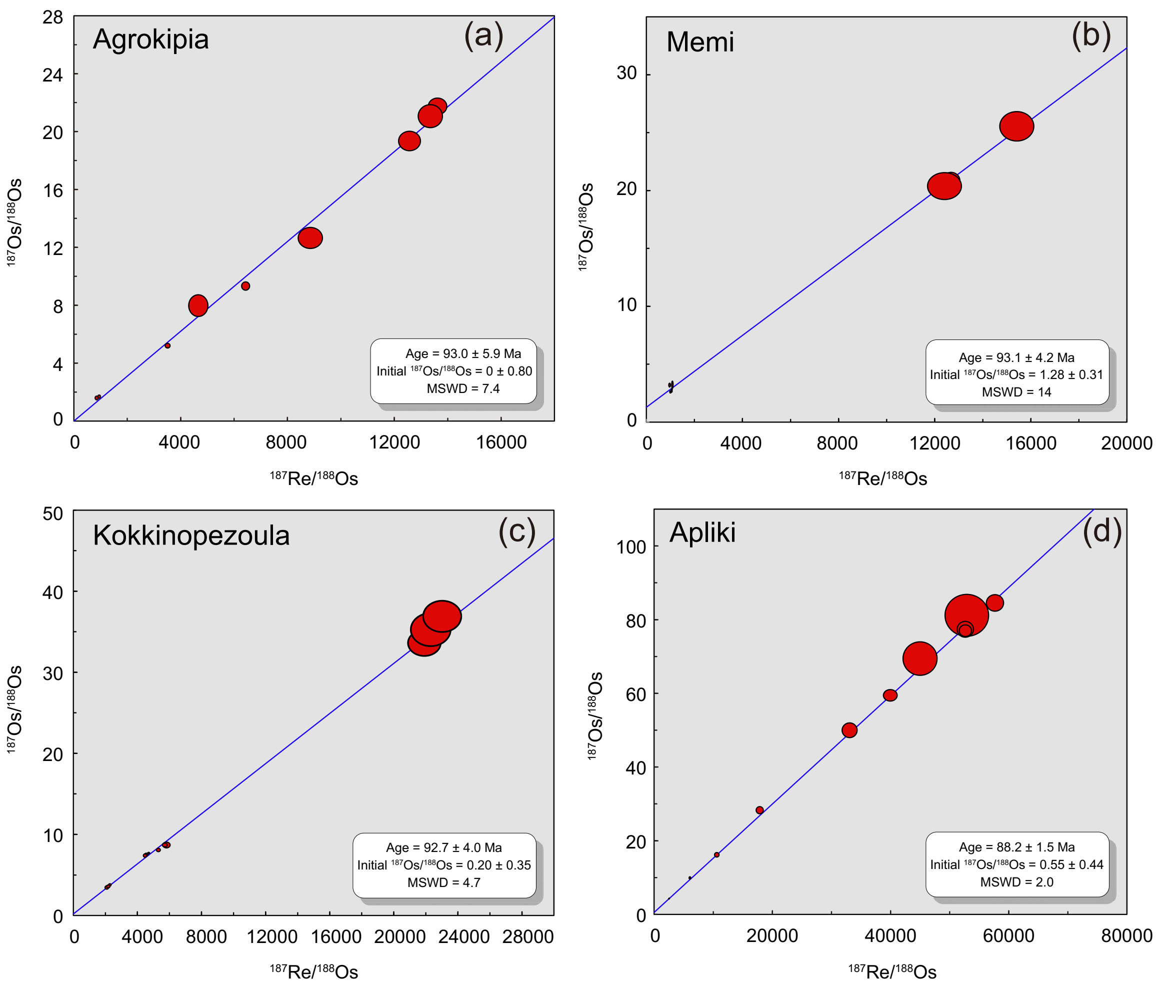

Figure 2 ^{187}Re/^{188}Os *versus* ^{187}Os/^{188}Os isochron diagrams for pyrite from four sulfide deposits in the Troodos ophiolite.

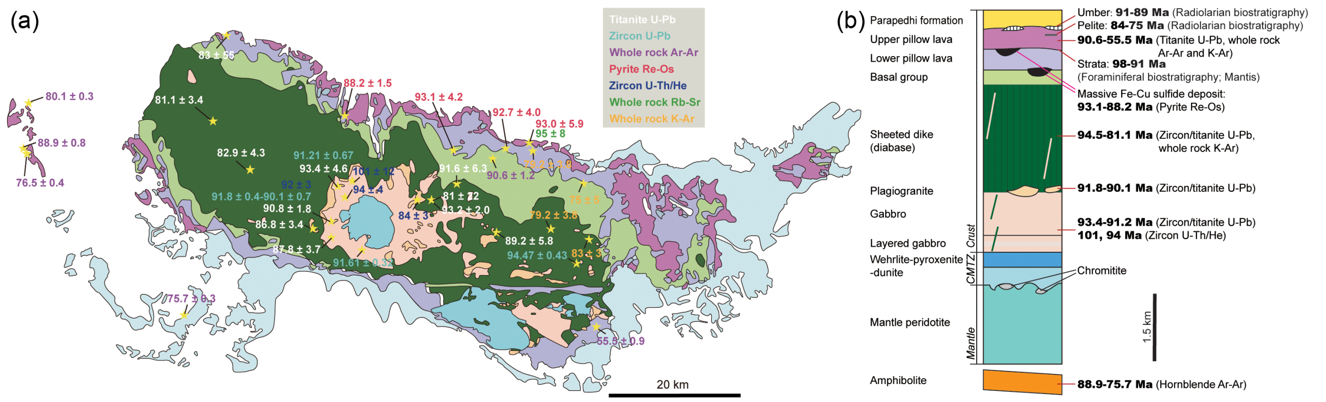

Figure 3 Compilation of age data reported for the Troodos ophiolite and their distribution in **(a)** geological map, and **(b)** schematic vertical profile. Data sources are available in Table S-2.

homogeneous fluid, (2) the Re-Os system remains closed after crystallisation (no gain/loss of Re or Os), and (3) sufficient spread exists in $^{187}Re/^{188}Os$ ratios for a statistically robust regression (Reisberg and Meisel, 2002; Li *et al.*, 2025).

In Troodos sulfide deposits, pyrite is the dominant sulfide mineral across all zones (massive ore, pyrite-quartz, and stockwork). The well preserved, low grade metamorphic character of the ophiolite, combined with syngenetic formation during axial hydrothermal activity and limited post-formation disturbance in many deposits (Constantinou and Govett, 1973; Richards *et al.*, 1989), satisfies the key requirements for reliable Re-Os isochron dating: cogenetic samples, closed system behaviour after crystallisation, and sufficient spread in parent/daughter ratios. Because pyrite in these deposits typically contains measurable common Os (0.0015–0.0864 ng/g, with one value of 0.8678 ng/g; Table S-1), multiple co-genetic pyrite separates from individual deposits can be analysed to construct a $^{187}Re/^{188}Os$ *vs.* $^{187}Os/^{188}Os$ isochron. Rigorous blank control (Re 3.0 ± 0.7 pg/g; Os 0.51 ± 0.13 pg/g; $^{187}Os/^{188}Os$ 2.719 ± 0.022; Supplementary Information) further enhances precision, achieving uncertainties of a few percent. As a consequence, the Re-Os dates from pyrite represent formation ages of these sulfide deposits. The data reliability is supported by consistent ages of 95 ± 8 Ma (whole rock Rb-Sr; Kawahata and Scott, 1990) and 93.0 ± 5.9 Ma (pyrite Re-Os; this study) for the Agrokipia deposit, and by slightly younger radiolarian biostratigraphy ages of 89–91 Ma of Umberiferous strata overlying the ophiolite (Blome and Irwin, 1985). The significant variability of initial $^{187}Os/^{188}Os$ ratios between the deposits (Fig. 2) is likely related to the sources of the hydrothermal fluids from which the pyrites formed, which has been revealed from studies of host rocks and deposits (Kawahata and Scott, 1990; Adamides, 2010; Fonseca *et al.*, 2017).

Reconstruction of the geochronological framework for the Troodos ophiolite. The complete Troodos ophiolite sequence is believed to preserve the entire hydrothermal system from root zone to seafloor discharge (Gillis and Robinson, 1990; Fonseca *et al.*, 2017). The sulfide deposits record the full history of axial high temperature mineralisation, sub-seafloor stockwork formation, preservation during crustal construction, and subsequent off axis low temperature alteration, providing a uniquely accessible "fossil" oceanic hydrothermal system (Richards *et al.*, 1989; Martin *et al.*, 2018). Consequently, the Re-Os isochron dates of these deposits can be integrated with recent high precision age data (Table S-2) to reconstruct the geochronological framework for the formation of the Troodos ophiolite.

1. Crustal accretion and high temperature mineralisation (~93–90 Ma). Zircon and titanite U-Pb dates from the plutonic section define the main construction phase of the Troodos ophiolite. Gabbro crystallisation is recorded at 93.4 ± 4.6 Ma, 91.6 ± 0.3 Ma, and 91.2 ± 0.7 Ma (Su *et al.*, 2025), while plagiogranites yield a tight cluster of 91.8 ± 0.4 Ma to 90.1 ± 0.7 Ma (Chen *et al.*, 2020; Mukasa and Ludden, 1987; Konstantinou *et al.*, 2007; Su *et al.*, 2025). Four diabase samples in the sheeted dike complex give zircon/titanite U-Pb dates of 94.5 ± 0.4 Ma to 89.2 ± 5.8 Ma (Su *et al.*, 2025), with the older end overlapping the ages of the gabbro-plagiogranite suite. These ages are spatially distributed across the central and southern Troodos Massif (Fig. 3a), confirming synchronous plutonism and dike injection.

The Re-Os isochron dates on pyrite from the three sulfide deposits (Fig. 2) overlap within uncertainty with the plutonic U-Pb dates and with a Rb-Sr whole rock date of 95 ± 8 Ma (Kawahata and Scott, 1990) for host rock at Agrokipia. They are stratigraphically consistent with foraminiferal biostratigraphy (98–91 Ma) in strata between Upper and Lower Pillow Lavas (Mantis, 1971) and radiolarian biostratigraphy (91–89 Ma) in umberiferous sediments of the Perapedhi Formation (Parapedhi unit) (Blome and Irwin, 1985). Whole rock Ar-Ar dating of arc tholeiite (90.6 ± 1.2 Ma; Osozawa *et al.*, 2012) further brackets volcanism. The stratigraphic column (Fig. 3b) places sulfide mineralisation precisely within the pillow lava sequence, contemporaneous with axial hydrothermal circulation.

2. Post-accretion low temperature overprint and cooling (~88–74 Ma). Rb-Sr dates on celadonite record off axis alteration from 86.1 ± 0.4 Ma (celadonite-zeolite vein; Staudigel *et al.*, 1986) to 76 ± 4 and 74 ± 5 Ma (whole rock; Laureijs *et al.*, 2021). Hornblende Ar-Ar dates from amphibolite soles (88.9 ± 0.8 to 75.7 ± 0.3 Ma; Chan *et al.*, 2007) reflect cooling or obduction related metamorphism. Whole rock K-Ar dates on pillow lavas, sheeted dikes, and andesites (84.7–75 Ma; Desmet *et al.*, 1978; Delaloye and Desmet, 1979; Delaloye *et al.*, 1980; Staudigel *et al.*, 1986) are interpreted as Ar loss or partial resetting during alteration. U-Th/He zircon dates (92–83 Ma; Morag *et al.*, 2016) track low temperature cooling shortly after formation.

3. Later magmatic events. Five diabase samples yield 87.8 ± 3.7 Ma to 81.1 ± 3.4 Ma (titanite U-Pb; Su *et al.*, 2025), suggesting long term magmatism since 94.5 Ma to form sheeted dikes. A depleted boninite sample yields a whole rock Ar-Ar date of 55.5 ± 0.9 Ma (Osozawa *et al.*, 2012), indicating minor post-ophiolite magmatism. Radiolarian ages in pelites interlayered with Upper Pillow Lavas (84–75 Ma; Desmet, 1977) suggest continued or renewed sedimentary/volcanic activity. The younger

Re-Os date (88.2 ± 1.5 Ma) and prominently higher Re and Os concentrations in pyrite from the Apliki deposit relative to the other three deposits (Table S-1) likely reflect compositional changes of magmas with time.

4. Spatial and stratigraphic coherence. Figure 3a shows the ~93–90 Ma cluster is widespread across the ophiolite, with younger magmatic ages in western part. The younger alteration ages are more peripheral or associated with fault zones. The idealised crustal column (Fig. 3b) integrates all data, demonstrating that high temperature sulfide mineralisation, volcanism, and plutonism were essentially synchronous during fast-to-intermediate spreading (Gillis and Robinson, 1990).

Conclusion and Implications

This study reports the first Re-Os isochron dates for pyrite from Cyprus-type VMS deposits in the Troodos ophiolite, yielding formation ages of ~93 Ma for Agrokipia, Memi, and Kokkinopezoula deposits, and a younger ~88 Ma for Apliki, although they overlap within uncertainty. Integrated with U-Pb, Ar-Ar, and Rb-Sr geochronological data, these ages allow us to reconstruct a comprehensive temporal framework for the formation and evolution of this classic ophiolite. The close temporal coincidence of plutonism, volcanism, and seafloor hydrothermal activity at ~93–90 Ma demonstrates that the main crustal construction phase of the Troodos ophiolite occurred during a short lived (~3 Myr), rapid spreading event.

Following the main phase of crustal accretion, the ophiolite experienced a prolonged thermal evolution lasting until ~74 Ma. Ages from amphibolite soles, celadonite, and low temperature thermochronology record progressive cooling and the onset of obduction related metamorphism. The ~15 Myr interval between initial crustal accretion and final cooling/obduction implies that the Troodos lithosphere remained in a regime with persistent hydrothermal circulation long after magmatism had ceased. This extended thermal history provides a valuable template for understanding the complete "life cycle" of young oceanic lithosphere in supra-subduction zone environments.

In addition, the Re-Os pyrite isochron dates highlight the utility of VMS deposits as precise chronometers for fossil seafloor hydrothermal systems. The ~93 Ma ages confirm that sulfide mineralisation was synchronous with axial volcanism and high temperature hydrothermal circulation, while the slightly younger ~88 Ma age at Apliki is consistent with evidence for later magmatism in the western part of the ophiolite. These findings demonstrate the potential of Re-Os geochronology on pyrite to resolve short duration magmatic-hydrothermal events in ancient oceanic crust.

Acknowledgements

We thank editor Romain Tartèse and reviewer Laurie Reisberg for their constructive comments, which significantly improved the quality of the paper. This study is funded by National Natural Science Foundation of China (42350001) and special fund of Deep Earth Probe and Mineral Resources Exploration-National Science and Technology Major Project of China (2025ZD1006104).

Editor: Romain Tartèse

Additional Information

Supplementary Information accompanies this letter at https://www.geochemicalperspectivesletters.org/article2629.

Cite this letter as: Su, B.-X., Gao, B.-Y., Ning, S., Symeou, V. (2026) Pyrite Re-Os dating confirms synchronous magmatism and hydrothermalism in Troodos ophiolite. *Geochem. Persp. Let.* 41, 29–34. https://doi.org/10.7185/geochemlet.2629

References

Adamides, N.G. (2010) Mafic-dominated volcanogenic sulphide deposits in the Troodos ophiolite, Cyprus Part 2 – A review of genetic models and guides for exploration. *Applied Earth Science* 119, 193–204. https://doi.org/10.1179/1743275811Y.0000000011

Blome, C.D., Irwin, W.P. (1985) Equivalent radiolarian ages from ophiolitic terranes of Cyprus and Oman. *Geology* 13, 401–404. https://doi.org/10.1130/0091-7613(1985)13<401:ERAFOT>2.0.CO;2

Chan, G.H.-N., Malpas, J., Xenophontos, C., Lo, C.-H. (2007) Timing of subduction zone metamorphism during the formation and emplacement of Troodos and Baer-Bassit ophiolites: insights from ^{40}Ar-^{39}Ar geochronology. *Geological Magazine* 144, 797–810. https://doi.org/10.1017/S0016756807003792

Chen, Y., Niu, Y., Shen, F., Gao, Y., Wang, X. (2020) New U-Pb zircon age and petrogenesis of the plagiogranite, Troodos ophiolite, Cyprus. *Lithos* 362–363, 105472. https://doi.org/10.1016/j.lithos.2020.105472

Constantinou, G., Govett, G.J.S. (1973) Geology, geochemistry, and genesis of Cyprus sulfide deposits. *Economic Geology* 68, 843–858. https://doi.org/10.2113/gsecongeo.68.6.843

Delaloye, M., Desmet, A. (1979) Nouvelles données radiométriques sur les pillow-lavas du Troodos (Chypre). "New radiometric data on the Troodos pillow lavas (Cyprus)." *Comptes Rendus de l'Académie des Sciences (D)* 288, 461–464.

Delaloye, M., Desmet, A., Desmons, J., Gagny, Cl., Rocci, G. (1980) Geochronological interpretation of the Troodos sheeted dike complex. *Ofioliti* 5, 27–34.

Desmet, A. (1977) *Contribution à l'étude de la croûte océanique mésozoïque de Méditerranée orientale: les pillow-lavas du Troodos (Chypre). "Contribution to the study of the Mesozoic oceanic crust of the Eastern Mediterranean: the Troodos pillow lavas (Cyprus)"*. Doctoral dissertation, Université de Nancy.

Desmet, A., Lapierre, H., Rocci, G., Gagny, Cl., Parrot, J.-F., Delaloye, M. (1978) Constitution and significance of the Troodos sheeted complex. *Nature* 273, 527–530. https://doi.org/10.1038/273527a0

Dilek, Y., Furnes, H. (2009) Structure and geochemistry of Tethyan ophiolites and their petrogenesis in subduction rollback systems. *Lithos* 113, 1–20. https://doi.org/10.1016/j.lithos.2009.04.022

Fonseca, R.O.C., Kirchenbaur, M., Ballhaus, C., Münker, C., Zirner, A., Gerdes, A., Heuser, A., Botcharnikov, R., Lenting, C. (2017) Fingerprinting fluid sources in Troodos ophiolite complex orbicular glasses using high spatial resolution isotope and trace element geochemistry. *Geochimica et Cosmochimica Acta* 200, 145–166. https://doi.org/10.1016/j.gca.2016.12.012

Geological Survey Department, Cyprus (2016) Geological map of Cyprus, 1:250,000.

Gillis, K.M., Robinson, P.T. (1990) Patterns and processes of alteration in the lavas and dykes of the Troodos Ophiolite, Cyprus. *Journal of Geophysical Research: Solid Earth* 95, 21523–21548. https://doi.org/10.1029/JB095iB13p21523

Kawahata, H., Scott, S.D. (1990) Strontium isotopes and water-rock interaction of the Agrokipia 'B' stockwork deposit in the Troodos ophiolite, Cyprus: a fossil subseafloor ore body. *Geochemical Journal* 24, 349–356. https://doi.org/10.2343/geochemj.24.349

Konstantinou, A., Wirth, K., Vervoort, J. (2007) U-Pb isotopic dating of Troodos plagiogranite, Cyprus by LA-ICP-MS. *Geological Society of America Annual Meeting*, Denver, 28–31 October 2007, Session 143, Paper 16.

Laureijs, C.T., Coogan, L.A., Spence, J. (2021) Regionally variable timing and duration of celadonite formation in the Troodos lavas (Cyprus) from Rb-Sr age distributions. *Chemical Geology* 560, 119995. https://doi.org/10.1016/j.chemgeo.2020.119995

Li, Y., Glorie, S., Selby, D. (2025) Re–Os geochronology for sulfides and organic-rich sediments. *National Science Review* 12, nwaf300. https://doi.org/10.1093/nsr/nwaf300

Mantis, M. (1971) Paleontological evidence defining the age of the Troodos pillow lava series. *Cypriakos Logos* 3, 202–208.

Martin, A.J., McDonald, I., MacLeod, C.J., Prichard, H.M., McFall, K. (2018) Extreme enrichment of selenium in the Apliki Cyprus-type VMS deposit, Troodos, Cyprus. *Mineralogical Magazine* 82, 697–724. https://doi.org/10.1180/mgm.2018.81

Moores, E.M., Robinson, P.T., Malpas, J., Xenophonotos, C. (1984) Model for the origin of the Troodos massif, Cyprus, and other mideast ophiolites. *Geology* 12, 500–503. https://doi.org/10.1130/0091-7613(1984)12<500:MFTOOT>2.0.CO;2

Morag, N., Haviv, I., Katzir, Y. (2016) From ocean depths to mountain tops: Uplift of the Troodos ophiolite (Cyprus) constrained by low-temperature thermochronology and geomorphic analysis. *Tectonics* 35, 622–637. https://doi.org/10.1002/2015TC004069

Mukasa, S.B., Ludden, J.N. (1987) Uranium-lead isotopic ages of plagiogranites from the Troodos ophiolite, Cyprus, and their tectonic significance. *Geology* 15, 825–828. https://doi.org/10.1130/0091-7613(1987)15<825:UIAOPF>2.0.CO;2

Osozawa, S., Shinjo, R., Lo, C.-H., Jahn, B.-m., Hoang, N., Sasaki, M., Ishikawa, K., Kano, H., Hoshi, H., Xenophontos, C., Wakabayashi, J. (2012) Geochemistry and geochronology of the Troodos ophiolite: An SSZ ophiolite generated by subduction initiation and an extended episode of ridge subduction? *Lithosphere* 4, 497–510. https://doi.org/10.1130/L205.1

Pearce, J.A., Robinson, P.T. (2010) The Troodos ophiolitic complex probably formed in a subduction initiation, slab edge setting. *Gondwana Research* 18, 60–81. https://doi.org/10.1016/j.gr.2009.12.003

Reisberg, L., Meisel, T. (2002) The Re-Os Isotopic System: A Review of Analytical Techniques. *Geostandards Newsletter* 26, 249–267. https://doi.org/10.1111/j.1751-908X.2002.tb00633.x

Richards, H.G., Cann, J.R., Jensenius, J. (1989) Mineralogical zonation and metasomatism of the alteration pipes of Cyprus sulfide deposits. *Economic Geology* 84, 91–115. https://doi.org/10.2113/gsecongeo.84.1.91

Robertson, A.H.F., Parlak, O., Tasli, K. (2024) Testing alternative tectonic models for the Permian-Pleistocene tectonic development of the Kyrenia Range, N Cyprus: Implications for E Mediterranean Tethyan palaeogeography. *Gondwana Research* 132, 343–379. https://doi.org/10.1016/j.gr.2024.05.003

Staudigel, H., Gillis, K., Duncan, R. (1986) K/Ar and Rb/Sr ages of celadonites from the Troodos ophiolite, Cyprus. *Geology* 14, 72–75. https://doi.org/10.1130/0091-7613(1986)14<72:AASAOC>2.0.CO;2

Stein, H.J., Morgan, J.W., Scherstén, A. (2000) Re-Os Dating of Low-Level Highly Radiogenic (LLHR) Sulfides: The Harnäs Gold Deposit, Southwest Sweden, Records Continental-Scale Tectonic Events. *Economic Geology* 95, 1657–1671. https://doi.org/10.2113/gsecongeo.95.8.1657

Su, B.-X., Wang, J., Pan, Q.-Q., Xiao, Y., Cui, M.-M. (2025) Impact-induced 'young' zircon in old rocks from Troodos ophiolite, Cyprus. *Journal of the Geological Society* 182, jgs2024-192. https://doi.org/10.1144/jgs2024-192

Whattam, S.A., Stern, R.J. (2011) The 'subduction initiation rule': a key for linking ophiolites, intra-oceanic forearcs, and subduction initiation. *Contributions to Mineralogy and Petrology* 162, 1031–1045. https://doi.org/10.1007/s00410-011-0638-z

Geochemical Perspectives Letters

Pyrite Re-Os dating confirms synchronous magmatism and hydrothermalism in Troodos ophiolite

B.-X. Su, B.-Y. Gao, S. Ning, V. Symeou

Supplementary Information

The Supplementary Information includes:

- Analytical Procedure of Re-Os Isochron Dating
- Tables S-1 and S-2
- Supplementary Information References

Analytical Procedure of Re-Os Isochron Dating

Rhenium-osmium isotopic analyses were conducted at Metallogenic Elements and Isotopes Lab in the Institute of Geology and Geophysics, Chinese Academy of Sciences. 1 g of sample was weighed and loaded in a Carius tube. The mixed ^{185}Re and ^{190}Os spike, 5 ml of 10 M HCl and 15 ml of 15 M HNO_3 were added while the bottom part of the tube was frozen at -80 °C to -50 °C in an ethanol-liquid nitrogen slush; and the top was sealed using an oxygen-propane torch. After 15 mins of ultrasonic oscillating the tube was then placed in a stainless-steel jacket and heated for 48 h at 220 °C. Upon cooling, the bottom part of the tube was kept frozen and the neck of the tube was broken. The Os was separated as OsO_4 from the inverse aqua regia solution by distillation in the steam bath, and trapped in 2 ml ice water for Os isotope ratio determination (Jin *et al*., 2013). The residual Re-bearing solution was evaporated to dryness at 80 °C and purified by solvent extraction method using $NH_3{\cdot}H_2O$-butanone (Gao *et al*., 2022). The Os and Re isotope ratios were determined using an inductively coupled plasma mass spectrometer (ICP-MS Element-XR). The reference material JCBY analyzed in this study yielded concentrations of 38.39 ± 0.26 ng/g for Re and 16.13 ± 0.20 ng/g for Os and $^{187}Os/^{188}Os$ ratio of 0.3389 ± 0.0056, in good agreement with the results in literature (38.61 ± 0.54 ng/g Re and 16.23 ± 0.17 ng/g Os, Qu *et al*., 2010; 0.33602 ± 0.00022 $^{187}Os/^{188}Os$, Qu *et al*., 2009). The four blanks yielded average concentrations of 3.0 ± 0.7 pg/g for Re and 0.51 ± 0.13 pg/g for Os and $^{187}Os/^{188}Os$ ratio of 2.719 ± 0.022 (1 s.d.). In radiogenic sulfides the blank-induced errors on $^{187}Os/^{188}Os$ and $^{187}Re/^{188}Os$ are strongly correlated, so they have little effect on the isochron slope (i.e., the age) (e.g., Stein *et al*., 2000; Li *et al*., 2025). Our samples have low common Os and high $^{187}Re/^{188}Os$ ratios (generally >1000). The blank mainly affects the initial $^{187}Os/^{188}Os$ intercept, not the slope.

Supplementary Tables

Table S-1 Re and Os isotope data of pyrite from four sulfide deposits in the Troodos ophiolite.

Sample	Re (ng/g)	2σ	Common Os (ng/g)	2σ	^{187}Os (ng/g)	2σ	^{187}Re/^{188}Os	2σ	^{187}Os/^{188}Os	2σ
Agrokipia deposit										
24TR-28-1	7.803	0.057	0.01132	0.00022	0.00755	0.00011	3524	76	5.22	0.13
24TR-28-2	6.776	0.054	0.00570	0.00009	0.00647	0.00011	6444	124	9.34	0.23
24TR-28-3	7.173	0.058	0.00453	0.00016	0.00673	0.00014	8867	371	12.67	0.59
24TR-29-1	1.657	0.016	0.00234	0.00011	0.00207	0.00008	4670	293	7.99	0.61
24TR-30-1	5.408	0.036	0.00254	0.00004	0.00572	0.00004	13633	283	21.76	0.46
24TR-30-2	5.268	0.037	0.00265	0.00005	0.00539	0.00006	12583	332	19.37	0.55
24TR-30-3	5.386	0.035	0.00257	0.00005	0.00563	0.00008	13363	370	21.08	0.65
24TR-31-1	0.613	0.005	0.00370	0.00013	0.00097	0.00002	956	40	1.69	0.09
24TR-31-2	0.587	0.004	0.00387	0.00018	0.00097	0.00002	868	47	1.61	0.10
Memi deposit										
24TR-45-1	2.900	0.025	0.00153	0.00003	0.00331	0.00005	15428	578	25.57	1.04
24TR-45-2	2.862	0.022	0.00171	0.00002	0.00325	0.00005	12693	300	20.87	0.58
24TR-45-3	2.850	0.020	0.00173	0.00005	0.00323	0.00002	12419	578	20.40	0.95
24TR-47-1	2.332	0.018	0.01224	0.00034	0.00506	0.00015	979	30	3.21	0.14
24TR-47-2	2.494	0.018	0.01190	0.00020	0.00442	0.00005	1068	21	2.82	0.06
24TR-47-3	2.441	0.016	0.01222	0.00028	0.00425	0.00007	1015	25	2.63	0.08
24TR-47-4	2.382	0.017	0.01147	0.00018	0.00407	0.00006	1060	20	2.68	0.06
24TR-47-5	2.444	0.021	0.01152	0.00022	0.00480	0.00035	1095	24	3.24	0.26
Kokkinopezoula deposit										
24TR-58-1	2.586	0.019	0.00297	0.00004	0.00276	0.00003	5325	98	8.10	0.17
24TR-58-2	2.429	0.024	0.00263	0.00006	0.00257	0.00003	5833	185	8.72	0.29
24TR-58-3	2.494	0.019	0.00273	0.00004	0.00268	0.00002	5729	121	8.72	0.19
24TR-59-1	9.373	0.071	0.01052	0.00016	0.01000	0.00008	4572	82	7.53	0.14
24TR-59-2	9.382	0.069	0.01070	0.00018	0.01001	0.00015	4496	85	7.41	0.17
24TR-59-3	9.355	0.065	0.01020	0.00008	0.00990	0.00004	4719	52	7.72	0.07
24TR-60-1	5.918	0.041	0.00193	0.00005	0.00600	0.00006	21930	835	33.65	1.31
24TR-60-2	5.423	0.039	0.00180	0.00005	0.00539	0.00008	22326	1013	35.30	1.67
24TR-60-3	5.483	0.039	0.00178	0.00005	0.00552	0.00006	23045	972	36.94	1.58
24TR-61-1	1.793	0.013	0.00473	0.00017	0.00215	0.00005	2104	89	3.47	0.17
24TR-61-2	1.839	0.014	0.00448	0.00010	0.00220	0.00004	2298	61	3.79	0.12
24TR-61-3	1.782	0.014	0.00454	0.00015	0.00213	0.00003	2195	85	3.60	0.15

Note: Re, ^{187}Os, and common Os concentration data are blank-corrected; ^{187}Os values represent total ^{187}Os.

Table S-1 continued.

Sample	Re (ng/g)	2σ	Common Os (ng/g)	2σ	^{187}Os (ng/g)	2σ	^{187}Re/^{188}Os	2σ	^{187}Os/^{188}Os	2σ
Apliki deposit										
24TR-4-1	70.88	0.51	0.00708	0.00036	0.06858	0.00064	53008	3013	81.26	4.64
24TR-4-2	70.88	0.48	0.00822	0.00039	0.06895	0.00090	45099	2348	69.51	3.70
24TR-4-3	65.23	0.44	0.05128	0.00092	0.06592	0.00105	6220	120	9.96	0.24
24TR-5-1	112.88	1.48	0.01716	0.00046	0.10721	0.00172	33200	1030	50.05	1.62
24TR-5-2	113.96	1.62	0.01447	0.00026	0.10665	0.00107	40082	948	59.54	1.27
24TR-6-1	333.49	2.24	0.02851	0.00054	0.30735	0.00295	57763	1190	84.62	1.84
24TR-6-2	331.51	2.33	0.03098	0.00062	0.30633	0.00311	52744	1134	77.47	1.76
24TR-6-3	331.61	2.25	0.03098	0.00044	0.30476	0.00258	52760	845	77.07	1.29
24TR-7-1	481.58	3.59	0.86784	0.00984	0.48532	0.00499	2682	36	4.30	0.07
24TR-7-2	48.34	0.36	0.08641	0.00118	0.04864	0.00054	2721	43	4.33	0.08
24TR-7-3	40.84	0.31	0.01157	0.00029	0.04067	0.00034	18017	495	28.34	0.78
24TR-7-4	39.34	0.30	0.01839	0.00048	0.03756	0.00055	10763	302	16.24	0.50

Note: Re, ^{187}Os, and common Os concentration data are blank-corrected; ^{187}Os values represent total ^{187}Os.

Table S-2 Compilation of age data from the Troodos ophiolite.

Rock	Dating method	Mineral/Whole rock	Age (Ma)	Error (Ma)	Data source
Umberiferous strata overlying ophiolite	Radiolarian biostratigraphy		89-91		Blome and Irwin, 1985
Pelite interlayered with upper pillows	Radiolarian biostratigraphy		75-84		Desmet, 1977
Strata between upper and lower pillows	Foraminiferal biostratigraphy		91-98		Mantis, 1971
Celadonite-zeolite vein	Rb-Sr	Mineral pair	86.1	0.4	Staudigel et al., 1986
Celadonite	Rb-Sr	Whole rock	74.0	5.0	Laureijs et al., 2021
Celadonite	Rb-Sr	Whole rock	76.0	4.0	Laureijs et al., 2021
Depleted boninite	Ar-Ar	Whole rock	55.5	0.9	Osozawa et al., 2012
Pillow lava	U-Pb	Titanite	83.0	55.0	Su et al., 2025
Pillow lava	K-Ar	Whole rock	75.0	5.0	Delaloye and Desmet, 1979
Altered rock (Agrokipia deposit)	Rb-Sr	Whole rock	95	8	Kawahata and Scott, 1990
Sulfide ore (Agrokipia deposit)	Re-Os	Pyrite	93.0	5.9	This study
Sulfide ore (Apliki deposit)	Re-Os	Pyrite	88.2	1.5	This study
Sulfide ore (Kokkinopezoula deposit)	Re-Os	Pyrite	92.7	4.0	This study
Sulfide ore (Memi deposit)	Re-Os	Pyrite	93.1	4.2	This study
Arc tholeiite	Ar-Ar	Whole rock	90.6	1.2	Osozawa et al., 2012
Andesite of the arc tholeiite suite	K-Ar	Whole rock	84.7	2.3	Staudigel et al., 1986

Table S-2 continued.

Rock	Dating method	Mineral/Whole rock	Age (Ma)	Error (Ma)	Data source
Sheeted dike	K-Ar	Whole rock	83.0	3.0	Delaloye et al., 1980
Sheeted dike	K-Ar	Whole rock	79.2	3.8	Desmet et al., 1978
Diabase	U-Pb	Zircon	94.5	0.4	Su et al., 2025
Diabase	U-Pb	Titanite	93.2	2.0	Su et al., 2025
Diabase	U-Pb	Titanite	91.6	6.3	Su et al., 2025
Diabase	U-Pb	Titanite	89.2	5.8	Su et al., 2025
Diabase	U-Pb	Titanite	87.8	3.7	Su et al., 2025
Diabase	U-Pb	Titanite	86.8	3.4	Su et al., 2025
Diabase	U-Pb	Titanite	82.9	4.3	Su et al., 2025
Diabase	U-Pb	Titanite	81.1	3.4	Su et al., 2025
Diabase	U-Pb	Titanite	81.0	22.0	Su et al., 2025
Plagiogranite	U-Pb	Zircon	91	0.4	Chen et al., 2020
Plagiogranite	U-Pb	Zircon	91.8	0.4	Chen et al., 2020
Plagiogranite	U-Pb	Zircon	90.1	0.7	Chen et al., 2020
Plagiogranite	U-Pb	Zircon	91.2	1.0	Mukasa and Ludden, 1987
Plagiogranite	U-Pb	Zircon	91.6	1.4	Mukasa and Ludden, 1987
Plagiogranite	U-Pb	Zircon	90.8	1.6	Konstantinou et al., 2007
Plagiogranite	U-Pb	Zircon	91.1	1.3	Konstantinou et al., 2007
Plagiogranite	U-Th/He	Zircon	83.0	3.0	Morag et al., 2016
Plagiogranite	U-Th/He	Zircon	92.0	3.0	Morag et al., 2016
Plagiogranite	U-Pb	Titanite	90.8	1.8	Su et al., 2025
Plagiogranite	U-Pb	Zircon	90.5	1.1	Su et al., 2025
Gabbro	U-Th/He	Zircon	101.0	12.0	Morag et al., 2016
Gabbro	U-Th/He	Zircon	94.0	4.0	Morag et al., 2016
Gabbro	U-Pb	Titanite	93.4	4.6	Su et al., 2025
Gabbro	U-Pb	Zircon	91.6	0.3	Su et al., 2025
Gabbro	U-Pb	Zircon	91.2	0.7	Su et al., 2025
Amphibolite	Ar-Ar	Hornblende	88.9	0.8	Chan et al., 2007
Amphibolite	Ar-Ar	Hornblende	80.5	0.3	Chan et al., 2007
Amphibolite	Ar-Ar	Hornblende	76.5	0.4	Chan et al., 2007
Amphibolite	Ar-Ar	Hornblende	75.7	0.3	Chan et al., 2007

Supplementary Information References

Blome, C.D., Irwin, W.P. (1985) Equivalent radiolarian ages from ophiolitic terranes of Cyprus and Oman. *Geology* 13, 401–404. https://doi.org/10.1130/0091-7613(1985)13<401:ERAFOT>2.0.CO;2

Chan, G.H.-N., Malpas, J., Xenophontos, C., Lo, C.-H. (2007) Timing of subduction zone metamorphism during the formation and emplacement of Troodos and Baer-Bassit ophiolites: insights from ^{40}Ar-^{39}Ar geochronology. *Geological Magazine* 144, 797–810. https://doi.org/10.1017/S0016756807003792

Chen, Y., Niu, Y., Shen, F., Gao, Y., Wang, X. (2020) New U-Pb zircon age and petrogenesis of the plagiogranite, Troodos ophiolite, Cyprus. *Lithos* 362–363, 105472. https://doi.org/10.1016/j.lithos.2020.105472

Delaloye, M., Desmet, A. (1979) Nouvelles données radiométriques sur les pillow-lavas du Troodos (Chypre). "New radiometric data on the Troodos pillow lavas (Cyprus)." *Comptes Rendus de l'Académie des Sciences (D)* 288, 461–464.

Delaloye, M., Desmet, A., Desmons, J., Gagny, Cl., Rocci, G. (1980) Geochronological interpretation of the Troodos sheeted dike complex. *Ofioliti* 5, 27–34.

Desmet, A. (1977) *Contribution à l'étude de la croûte océanique mésozoïque de Méditerranée orientale: les pillow-lavas du Troodos (Chypre). "Contribution to the study of the Mesozoic oceanic crust of the Eastern Mediterranean: the Troodos pillow lavas (Cyprus)".* Doctoral dissertation, Université de Nancy.

Desmet, A., Lapierre, H., Rocci, G., Gagny, Cl., Parrot, J.-F., Delaloye, M. (1978) Constitution and significance of the Troodos sheeted complex. *Nature* 273, 527–530. https://doi.org/10.1038/273527a0

Gao, B., Li, W., Chu, Z., Zhang, L. (2022) An improved solvent extraction procedure for Re isotopic measurements. *Microchemical Journal* 180, 107568. https://doi.org/10.1016/j.microc.2022.107568

Jin, X., Li, W., Xiang, P., Sakyi, P.A., Zhu, M., Zhang, L. (2013) A contribution to common Carius tube distillation techniques. *Journal of Analytical Atomic Spectrometry* 28, 396–404. https://doi.org/10.1039/C2JA10374E

Kawahata, H., Scott, S.D. (1990) Strontium isotopes and water-rock interaction of the Agrokipia 'B' stockwork deposit in the Troodos ophiolite, Cyprus: a fossil subseafloor ore body. *Geochemical Journal* 24, 349–356. https://doi.org/10.2343/geochemj.24.349

Konstantinou, A., Wirth, K., Vervoort, J. (2007) U-Pb isotopic dating of Troodos plagiogranite, Cyprus by LA-ICP-MS. *Geological Society of America Annual Meeting*, Denver, 28–31 October 2007, Session 143, Paper 16.

Laureijs, C.T., Coogan, L.A., Spence, J. (2021) Regionally variable timing and duration of celadonite formation in the Troodos lavas (Cyprus) from Rb-Sr age distributions. *Chemical Geology* 560, 119995. https://doi.org/10.1016/j.chemgeo.2020.119995

Li, Y., Glorie, S., Selby, D. (2025) Re–Os geochronology for sulfides and organic-rich sediments. National Science Review 12, nwaf300. https://doi.org/10.1093/nsr/nwaf300

Mantis, M. (1971) Paleontological evidence defining the age of the Troodos pillow lava series. *Cypriakos Logos* 3, 202–208.

Morag, N., Haviv, I., Katzir, Y. (2016) From ocean depths to mountain tops: Uplift of the Troodos ophiolite (Cyprus) constrained by low-temperature thermochronology and geomorphic analysis. *Tectonics* 35, 622–637. https://doi.org/10.1002/2015TC004069

Mukasa, S.B., Ludden, J.N. (1987) Uranium-lead isotopic ages of plagiogranites from the Troodos ophiolite, Cyprus, and their tectonic significance. *Geology* 15, 825–828. https://doi.org/10.1130/0091-7613(1987)15<825:UIAOPF>2.0.CO;2

Osozawa, S., Shinjo, R., Lo, C.-H., Jahn, B.-m., Hoang, N., Sasaki, M., Ishikawa, K., Kano, H., Hoshi, H., Xenophontos, C., Wakabayashi, J. (2012) Geochemistry and geochronology of the Troodos ophiolite: An SSZ ophiolite generated by subduction initiation and an extended episode of ridge subduction?. *Lithosphere* 4, 497–510. https://doi.org/10.1130/L205.1

Qu, W.J., Du, A.D., Li, C., Sun, W.J. (2009) High-precise determination of osmium isotopic ratio in the Jinchuan copper-nickel sulfide ore samples. *Rock And Mineral Analysis* 28, 219–222 (in Chinese with English abstract).

Qu, W.J., Du, A.D., Yang, G., Li, C., Stein, H.J., Hannah, J.L. (2010) Re-Os reference material: JCBY and CORO. *Mineral Deposits* 29, 831–832 (in Chinese with English abstract).

Staudigel, H., Gillis, K., Duncan, R. (1986) K/Ar and Rb/Sr ages of celadonites from the Troodos ophiolite, Cyprus. *Geology* 14, 72–75. https://doi.org/10.1130/0091-7613(1986)14<72:AASAOC>2.0.CO;2

Stein, H.J., Morgan, J.W., Scherstén, A. (2000) Re-Os Dating of Low-Level Highly Radiogenic (LLHR) Sulfides: The Harnäs Gold Deposit, Southwest Sweden, Records Continental-Scale Tectonic Events. *Economic Geology* 95, 1657–1671. https://doi.org/10.2113/gsecongeo.95.8.1657

Su, B.-X., Wang, J., Pan, Q.-Q., Xiao, Y., Cui, M.-M. (2025) Impact-induced 'young' zircon in old rocks from Troodos ophiolite, Cyprus. *Journal of the Geological Society* 182, jgs2024-192. https://doi.org/10.1144/jgs2024-192